Cellulose **11:** 463–474, 2004.

Formation of nematic ordered cellulose and chitin

Tetsuo Kondo[1,*], Wakako Kasai[1] and R. Malcolm Brown, Jr.[2]
[1]*Graduate School of Bioresources and Bioenvironmental Science, Lab of Biomacromolecular Materials, Kyushu University, 6-10-1 Hakozaki, Higashi-ku, Fukuoka 812-8581, Japan*; [2]*School of Biological Sciences, Section of Molecular Genetics and Microbiology, University of Texas at Austin, Austin, TX 78712, USA*; **Author for correspondence (e-mail: tekondo@agr.kyushu-u.ac.jp)*

Received 22 December 2003; accepted in revised form 6 April 2004

Key words: α-Chitin, Cellulose, Nematic ordered cellulose, Orientation, Self-assembly, Stretching

Abstract

We proposed in a previous paper a unique form of β-glucan association, nematic ordered cellulose (NOC) that is molecularly ordered, yet non-crystalline. NOC has unique characteristics; in particular, its surface properties provide with a function of tracks or scaffolds for regulated movements and fiber-production of *Acetobacter xylinum* [Kondo et al. 2002. Proc. Natl. Acad. Sci. USA 99: 14008–14013]. In order to extend the usage of this NOC film as a functional template, the present article attempts to clarify how β-glucan association is initiated and established by uniaxial stretching of water swollen cellulose gel films. Wide angle X-ray diffraction, high-resolution transmission electron microscopy and atomic force microscopy were employed to exhibit molecular behavior of the ordering at various scales. Then, the preparative method for NOC was applied to the other carbohydrate polymers such as α-chitin and cellulose/α-chitin blends, leading to nematic ordered states as well as cellulose. However, the method did not necessarily provide the typical structure like NOC at the molecular scale. Instead, it yielded a variety of hierarchical nematic ordered states at various scales, which allows development of new artificial ordered sheet structures.

Introduction

In the native system, biosynthesized cellulose, which is a β-1,4-linked glucan homopolymer and the major polymer of plant cell walls, is extruded from complexes of enzymes called terminal complexes (TCs) on the plasma membrane, and then self-assembled leading to crystalline fibers. Namely, the TCs play a role as the nozzle-like tubes that synthesize and then extrude cellulose molecular chains for the molecular orientation (Kageyama et al. 1999). This entire system following the biosynthesis of the macromolecular chains is considered to be an oriented crystallization process.

Considering the above, the molecular ordering or orientation should be a key for consideration of the supermolecular structure on how the β-glucan chains associate. In our previous paper (Kondo et al. 2001), we showed that the predominant crystalline state of cellulose is included as a component in the ordered state. The major significance was that the ordered state also contains non-crystalline ordered states. This expanded the concept of how various states of molecular association could be categorized in cellulose. Finally, we proposed a novel type of glucan chain association termed nematic ordered cellulose (NOC). The structure is highly ordered but not crystalline, and could be created by induction of a specific drawing stress from a highly water-swollen cellulose (Togawa and Kondo 1999; Kondo et al. 2001). The NOC produces unique scattering patterns in X-ray diffraction in both equatorial and meridional axes, indicating that the direction of the molecules tends

to be parallel. The NOC structure is artificially made, however, this structure may be related to the possibility of 'paracrystalline domains' that has been discussed, which may exhibit a certain order in cellulose microfibrils of plant cell walls (Wardrop 1964; Harada and Côté 1985).

Further, this non-crystalline, yet ordered state in the NOC structure may provide exclusive properties as a material product over the native form of crystalline cellulose. *Acetobacter xylinum*, a Gram-negative bacterium, is well known to synthesize and extrude a ribbon of cellulose microfibrils, causing random movements. Recently, NOC surface as a template was found to control the deposition of the biosynthesized nanofibers epitaxially, by regulating the movements along the molecular orientation (molecular tracks). The simultaneous regulation of both the movements and the deposition of the nanofibers was triggered by the strong interaction between the nascent nanofibrils and the ordered molecules on the NOC template (Kondo et al. 2002). This unique relationship between directed biosynthesis and the ordered fabrication from the nano- to the micro-scales is expected to lead to new methodologies for the design of functional materials with desired nanostructures. More recently, the NOC has been revealed to exhibit totally different surface characteristics as well as the entire film when compared with conventional cellulose films; for example, fairly hydrophobic features and unique mechanical properties, which will be reported in a future paper. Therefore, further detailed investigation on NOC and in particular, the structure and property relationship has been required.

In this article, we have at first investigated changes in states of β-glucan chain association of stretched films midway to NOC structure using X-ray diffraction analyses, transmission electron microscopy (TEM) and atomic force microscopy (AFM), and then extended to the preparation method for the nematic ordered structure of both α-chitin and cellulose/α-chitin blends.

Experimental

Materials

Bleached cotton linters with a degree of polymerization (DP) of 1300 were used as the starting cellulose sample. α-Chitin samples were provided by Katakura Chikkarin Co. Ltd., and purified according to a previous paper (Saito et al. 1995). The cellulose and chitin were first dried under vacuum at 40 °C. *N*,*N*-Dimethylacetamide (DMAc) purchased from Katayama Chemicals Co. Ltd. (99 + %) was dehydrated with molecular sieve 3A and used without further purification. Lithium chloride (LiCl) powder (Katayama Chemicals Co. Ltd.) was oven-dried at least for 3 days at 105 °C.

Sample preparation

Water-swollen films from the DMAc/LiCl solution
Dissolution of cellulose and α-chitin and the subsequent preparation of water-swollen gel films were basically followed by a previous swelling procedure using a solvent exchange technique (Togawa and Kondo 1999; Kondo et al. 2001).

LiCl dried at 105 °C was dissolved in anhydrous DMAc to give a concentration of 5% (w/w) solution. Prior to swelling, the sample was disintegrated into fragments or small pieces by a mechanical disintegrator and dispersed into water which increased the surface area, making it easier to dissolve. The treated sample was soaked in water overnight, then squeezed and filtered to remove the water. It was then immersed in methanol, and again squeezed and filtered to remove excess methanol. After four repetitions of the methanol treatments, an exchange with acetone was performed once. Following the treatments with water, methanol, and acetone described above, the sample was solvent-exchanged with DMAc twice in the same procedure and soaked in the same solvent overnight. Another two repetitions of the above soaking and squeezing treatments with DMAc treatments were performed on the sample. Following the final squeeze, the sample was ready to be dissolved. The cellulose and α-chitin swollen by DMAc were dissolved in the DMAc/LiCl solution with constant stirring at room temperature, and at most 3 weeks' stirring was required to yield a transparent cellulose solution with a high viscosity. When the viscosity did not increase any more in the solution or suspension even after a week of stirring, 1–3% LiCl was added to allow complete dissolution, and then it was heated up to 50–60 °C for several hours. The

resulting solution was then centrifuged and filtered to remove any insoluble portion. The actual concentration (wt%) of the sample in the solution was determined by weighing a small portion of the dried film.

The slow coagulation to prepare the gel-like film from a DMAc/LiCl solution was carried out as follows. The solution was poured into a surface-cleaned glass Petri dish with a flat bottom and placed in a closed box containing saturated water vapor at room temperature. In this manner, saturated water vapor slowly diffused into the solution and precipitated the sample. The sample was allowed to stand at room temperature for several days until the precipitation under a saturated water vapor atmosphere was sufficiently complete to obtain the gel-like film. The precipitated and transparent gel-like film was washed with running distilled water for several days to remove the solvent, and a water-swollen gel-like film that was still transparent was obtained. The films were stored in water until needed.

Preparation of NOC and α-chitin films from water-swollen gel films

Nematic ordered films were prepared by stretching water-swollen gel-like films as prepared above. These films were cut into strips approximately 30 mm long and 5 mm wide. These water-swollen strips were then clamped in a manual stretching device and elongated uniaxially to a drawn ratio of 2.0 at room temperature. They were also stretched at the desired drawn ratio between 1.0 and 2.0 in order to obtain information on the molecular arrangements during the stretching. The entire drawing process was completed while the specimen was still in a wet state. Following air-drying, the drawn specimen in the stretching device was vacuum-dried at 40–50 °C for more than 24 h. The thickness of the dried films for X-ray measurements was about 80 μm.

Measurements

X-ray diffraction

X-ray diffraction measurements were basically performed according to our previous report (Togawa and Kondo 1999). Wide angle X-ray diffraction (WAXD) patterns were taken by a transmission method using Ni filtered CuKα radiation produced by a Rigaku RINT-2500HF X-ray generator. WAXD intensity curves were measured at 40 kV and 200 mA with scanning speed 0.5 °/min and scan step 0.02°. WAXD patterns were also recorded on an imaging plate (Fuji Film BAS-SR, 127 mm × 127 mm) at 40 kV and 60 mA for 10 min with a camera length of 60 mm, then analyzed with a Rigaku R-AXIS-DS3 system.

The WAXD intensity curves with a scanning speed of 0.5 °/min were measured by a transmission method using a scintillation counter at 40 kV and 200 mA through the angular range 2θ for the equatorial and the meridional scans to the drawing direction; $2\theta = 5$–$35°$ and 10–80°, respectively. Instrumental broadening was corrected using Si powder as a standard. The crystallinity index from the WAXD intensity curve was calculated assuming that the area ratio was given by the crystalline region area divided by the total area. To avoid complications due to contributions from the orientation in this measurement, the sample was cut into small pieces (a coarse powder) that were placed in a 1 mm glass capillary tube.

Transmission electron microscopy

For sample specimens examined by high-resolution TEM, the cellulose solutions were prepared in the same way as described above and diluted 100 times with water-free DMAc (1.0×10^{-2} wt%). After the solution covered a 3.0 mm TEM grid without coating, the grid was left for more than 3 days at room temperature under a saturated water vapor. During this period, a cellulose or α-chitin gel-like film was precipitated and at the same time was naturally stretched across the 3.0 mm diameter of the TEM grid during the drying process. It was then washed thoroughly with distilled water to exchange the solvent prior to the addition of the negative stain (aqueous 2% uranyl acetate) and finally air-dried. Interaction with uranyl acetate appears to protect samples from electron beam damage (Kondo et al. 2001). Specimens were observed with a Philips EM 420 transmission electron microscope operated at 100 kV with a beam current less than 5 μA. TEM images were acquired at magnifications of 210K and 450K using a GATAN Model 622 camera. The magnification factor for conversion to the digital image was 23×. The images were digitized, saved, and processed by Image Pro Plus software v.4.1 (Media Cybernetics).

Atomic force microscopy (AFM)

AFM images of the cellulose film specimens were acquired on a Nanoscope IIIa (Digital Instruments) microscope. AFM was performed at room temperature, being controlled in contact (DC) mode with a scan rate from 1 to 3 Hz to observe $1 \times 1\,\mu m^2$ areas. The AFM tip employed was an etched-silicon AFM tip with a nominal radius from 5 to 15 nm, a cone angle of 35° and a height of about 15 μm which was mounted on a rectangular type cantilever with a spring constant of 0.13 N m^{-1}. The scanning was carried out in both directions of the stretching axis and perpendicular to the axis of the film. The width and height of the aggregates was measured using a cross-sectional line profile analysis. Since the width data included geometrical enhancement due to the tip radius, they can be corrected using an equation introduced previously (Kondo 1999). In our case, as the height of the aggregates was smaller than the radius of the tip, the following correction equation was employed:

$$E = 2 \times (RH - H^2 1/2, \quad w = W - E,$$

where E is the geometrical enhancement on the real width value (w), W the apparent width observed in AFM, H the height of the object observed in AFM, and R is the AFM tip radius. In this study we employed an R value of 10 nm in radius.

Results and discussion

At first, we attempted to clarify changes in states of β-glucan chain association in midway to NOC structure using WAXD analyses, transmission electron microscopy and AFM. Then, the preparative method for NOC was applied to α-chitin and cellulose/α-chitin blends.

WAXD analyses of cellulose samples during the stretching process

Water-swollen gel-like films formed after slow coagulation and the subsequent solvent-exchange were transparent and composed of approximately 93 wt% of water and 7 wt% of cellulose prior to stretching. When stretching the water-swollen film uniaxially, drops of water extruded from the film as the orientation of the film increased. To understand the molecular ordering occurring during the stretching, the films stretched at the changing drawing ratio were provided for WAXD measurements. Figure 1 shows WAXD photographs of the fiber structure. It suggests that the undrawn films after being dried in a stretching device showed some orientation by natural shrinking, and with increasing drawing ratio of the samples, the rings were becoming arcs at the equatorial direction. To understand the details of the change, WAXD intensity curves were employed in both equatorial (Figure 2 – left) and meridional (Figure 2 – right) directions of the stretched film with the desired drawing ratio. Through the series, the present results derived from both reflections demonstrate that our stretched samples were highly ordered but remained non-crystalline, which gives a totally different profile when compared with that of cellulose II crystalline fibers (Togawa and Kondo 1999; Kondo et al. 2001). In the equatorial diffractions, the single reflection peak with the plane distance of 4.33 Å (at the peak top) got sharpened with increase in the drawn ratio. The meridional scan of WAXD was employed to analyze the order along the fiber direction for the stretched sample. In general, meridional intensities of cellulose are affected by the disorder of the neighboring chains that is symmetrical for the chain axis. As shown in Figure 2 (right), the meridional diffraction intensity pattern also shows narrowing of the reflection peaks accompanying the increase in the drawing ratio. These results indicate that the molecules were arranged to order parallel with a distance of 0.4–0.6 nm by stretching, similarly to the value of 0.66 nm obtained by the TEM analyses in a previous report (Kondo et al. 2001). However, the coordinates of the location of glucose residues may not be periodical along the stretching axis among the parallel molecular chains, as many reflections appeared in the meridional direction shown in Figure 2 (right). It should be noted as a reference that cellulose II crystalline fibers exhibit mainly two strong distinct reflections of the (002) and (004) planes in the corresponding direction, because glucan residues localized in cellulose II crystalline structure are quarter-staggered between the center and the corner chains along the longitudinal axis in the unit cell.

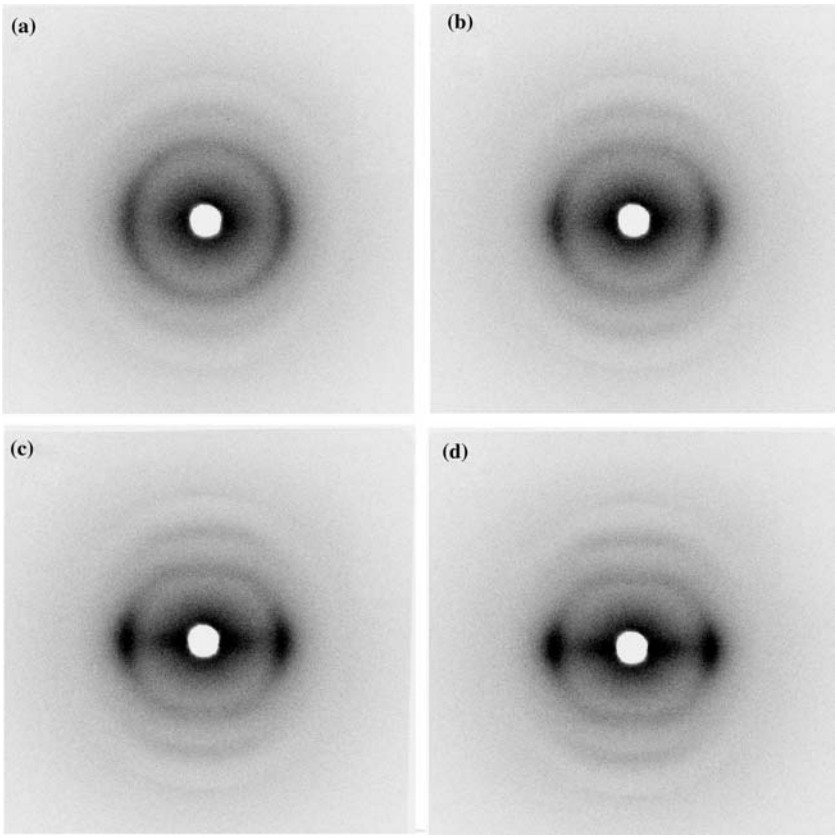

Figure 1. WAXD photographs for stretched cellulose films at the desired drawn ratio: (a) undrawn water-swollen film after being dried at a fixed state; (b) drawn ratio 1.5; (c) drawn ratio 1.7; and (d) drawn ratio 2.0.

When the drawn ratio reached 2.0, the orientation parameter calculated from WAXD photographs (Figure 1d) became 0.88, indicating a high degree of orientation. In this case, the structure is termed as NOC (Kondo et al. 2001). However, in NOC the relative crystallinity did not significantly follow the increase of the orientation by stretching, but remained at 16.8%. The characteristics are considerable line broadening of the meridional reflections in the profile of the NOC. This indicates that the structure of the nematic ordered cellulose film may have a certain disorder along the chain

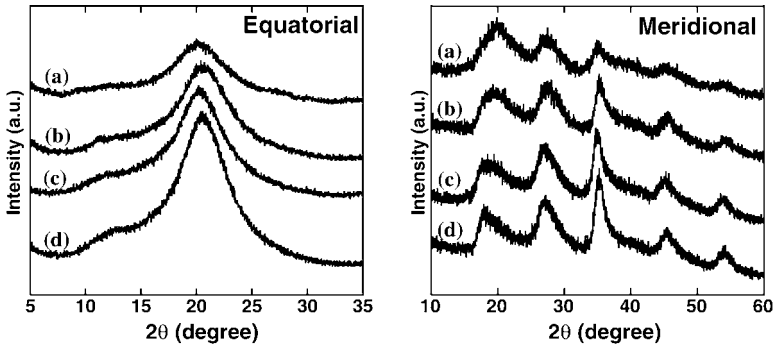

Figure 2. Equatorial (left) and meridional (right) intensity curves of the WAXD for cellulose films stretched at the desired drawn ratio corresponding to (a)–(d) in Figure 1. The term 'a.u.' indicates arbitrary unit.

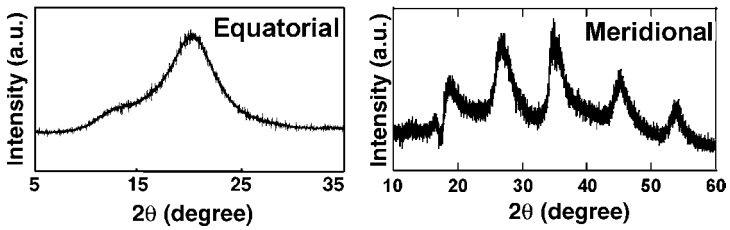

Figure 3. Calibrated equatorial (left) and meridional (right) intensity curves of the WAXD for the NOC film.

direction, which causes the ordered, but non-crystalline regions. Considering the crystallinity of the film sample (16.8%: crystallinity index calculated by X-ray diffraction measurements), the meridional direction profile should contain the contribution due to cellulose II crystals. Thus, the contribution of the crystallite was subtracted from the meridional direction profile in Figure 2d (right), and now the calibrated equatorial and meridional reflections in NOC are shown in the left and right parts of Figure 3, respectively.

Transitional molecular states leading to the ordered structure in NOC

It should be noted that X-ray diffraction patterns showed molecular orientation in the drawn samples, so parallel to the X-ray diffraction, we wanted to learn if it might be possible to image these orienting processes of glucan chains at the molecular level.

Using high-resolution TEM techniques, we determined the glucan chain associations in the stretching process of cellulose water-swollen gels. All specimens were negatively stained with uranyl acetate. The glucan chains appear to be decorated with the uranium (induced from uranyl acetate for the negative staining in the sample chamber of TEM), allowing them to be imaged as white dots or lines in the photographs (Kondo et al. 2001). Figure 4 ((a)–(c)) shows images of individual β-glucan chains in the process of molecular ordering. Before stretching of water-swollen cellulose gel films in Figure 4a, junction zones aggregating with a few glucan chains possibly by hydrogen bonding

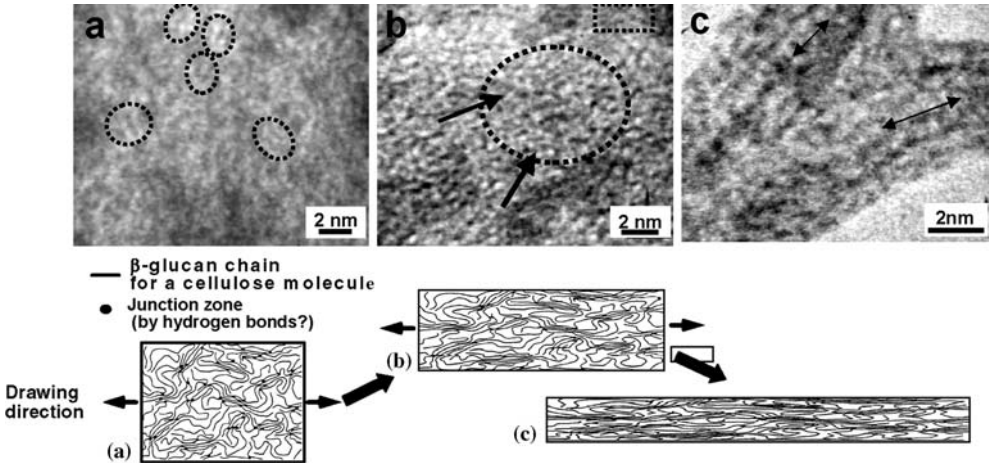

Figure 4. HRTEM images of single β-glucan chains in transitional molecular states leading to the ordered structure in NOC during the stretching process. (a) Non-ordered state where the hydrogen bonded junction zones (the dotted circle) exist; (b) transitional molecular states leading to the ordered structure (the arrows indicate the ordering direction and the circle indicates the initiated ordering of molecular parallel arrangements), and (c) ordered, non-crystalline regions of the stretched NOC. The sample on the grid was negatively stained with 2% uranyl acetate. Interaction with uranyl acetate appears to protect samples from electron beam damage. The dotted rectangular circle in (b) indicates the 0.24 nm uranium orthorombic crystalline lattice that proves well resolved with a minimum of astigmatism. The scale bar indicates 2 nm.

(the dotted circles) may be present as an ordered structure (Kondo and Sawatari 1996; Hishikawa et al. 1999). When the samples are uniaxially stretched at molecular scales, some points for the action such as hydrogen bonding networks and entanglements are required to transfer the physical force to individual molecules (Matsuo et al. 1985). Thus, the dotted circles in the image (a) may correspond to the schematic representation (a) in Figure 4. When the sample was stretched, the individual molecules initiated to be self-ordered along the stretching direction (the arrows in image (b)), and tended to form a parallel orientation (the dotted circles in image (b)). Finally, the ordered state as the NOC was established as shown in image (c). The behavior shown in images (b) and (c) is also drawn in the schematic representations (b) and (c) in Figure 4. In this way, these TEM images exhibit a typical molecular chain ordering of cellulose in the water-swollen gels as generally believed in the occurrence of molecular orientation when drawing a film.

Now, what happened to the junction zones that would enhance the transfer of stretching force to the individual molecules? Figure 5 shows the TEM image of a junction zone where individual molecules are associated to one another. The junction zone was located between molecular chains' ordered areas in the nematic ordered sample as illustrated in the schematic drawing of the same figure. In Figure 5, it should be noted that the 0.24 nm uranium orthorombic crystalline lattice appears clearly, which proves that uranium decorates the glucan chains to protect them from electron beam damage, and also well resolved with a minimum of astigmatism. Thus, as we expected, these TEM images shown in Figures 4 and 5 indicate that the physical force due to stretching may transfer to individual molecules by junction zones, which initiates the molecular chain orientation leading to the NOC state.

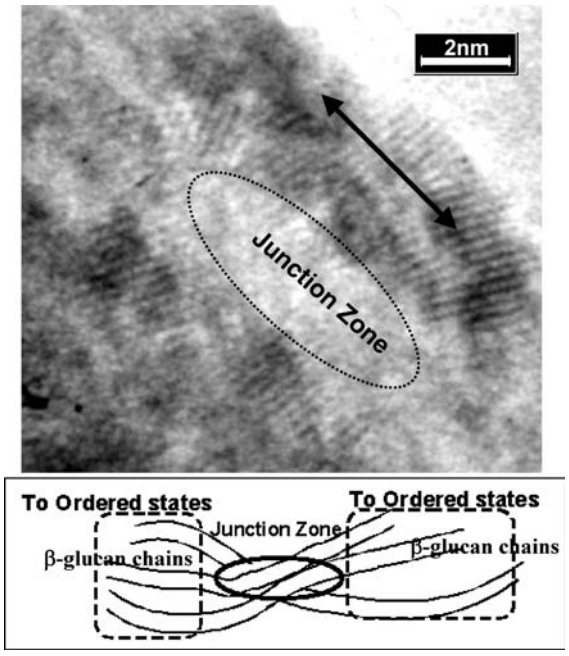

Figure 5. HRTEM image in the electron micrograph for a junction zone of glucan chains with a schematic drawing of aggregation of a single β-glucan chain. The dotted circle indicates the junction zone. Scale bar indicates 2 nm. The double arrow indicates the stretching direction.

Change of surface morphology of the samples during the transitional states leading to the NOC

We employed the same specimens used for X-ray diffraction analyses to provide for AFM analyses in order to examine change in the surface morphology of our cellulose samples obtained by uniaxially stretching highly water-swollen film at the desired drawing ratio. It was almost impossible to observe molecular images of the film surfaces with a low drawing ratio using high resolution AFM, because the surface of the specimens was too flexible for AFM tips to approach. Therefore, this AFM observation was limited to a 1-μm^2 scale. AFM images and the cross-section of the surface of the cellulose films shown in Figure 6A–D demonstrate that well-aligned molecular aggregates with a width of a few 10 nm and a height of 3–4 nm on average were becoming oriented uniaxially as the drawing ratio increased. In Table 1 is shown that, as the stretching proceeded, the average distance between two parallel lines (=molecular aggregates) became narrower. The standard deviation was also remarkably decreased following the change in the average distance. This indicates clearly that molecular aggregates were becoming better aligned on the film surface with increase of the molecular orientation due to the uniaxial stretching. On the other hand, the height was not significantly changed with increase in the drawing ratio. It should be noted that the surface roughness of the stretched films was fairly smooth when compared with other polymer films.

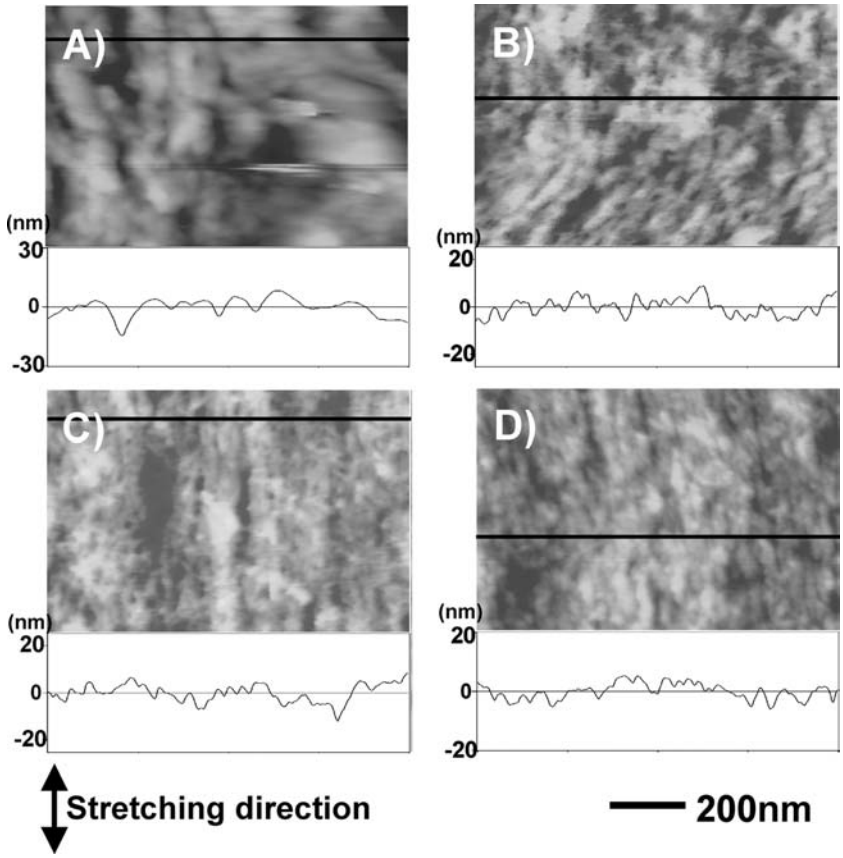

Figure 6. AFM images of height mode with the cross-section for cellulose films stretched at the desired drawn ratio corresponding to (a)–(d) in Figure 1. (A) Undrawn water-swollen film after being dried at a fixed state; (B) drawn ratio 1.5; (C) drawn ratio 1.7; and (D) drawn ratio 2.0. The scale bar indicates 200 nm.

Nematic ordered α-chitin and cellulose/α-chitin blends

Nematic ordered α-chitin

Figure 7 shows high-resolution TEM images of molecular assembly in the stretched samples of α-chitin and cellulose/α-chitin blend with a composition of 25/75 that were prepared in the same manner as for NOC. They exhibited occurrence of the orientation of molecular aggregation as seen in white lines, but were not resolved at the individual molecular chain scale, unlike the high-resolution TEM image of NOC (Kondo et al. 2001). By image analyses of the two TEM photographs in Figure 7, the average width and distance between two parallel lines were obtained as listed in Table 2

Table 1. The average distance[a] and height between two parallel lines obtained by analyses of AFM images (nm).

Drawing ratio	Cellulose		Cellulose/α-chitin (50/50)	
	Distance	Height	Distance	Height
1.0	Uncountable	Uncountable	Uncountable	Uncountable
1.5	28.9 ± 12.6	3.7 ± 2.0	21.9 ± 5.3	1.9 ± 1.0
1.7	27.9 ± 8.3	3.1 ± 1.6	20.0 ± 2.7	2.0 ± 0.9
2.0	23.6 ± 5.6	3.0 ± 1.1	25.1 ± 5.1	2.6 ± 0.9
	α-Chitin			
2.0	21.9 ± 5.3	3.7 ± 1.5		

[a]The average distance was calculated on the basis of calibrated data according to the equation in the Experimental section.

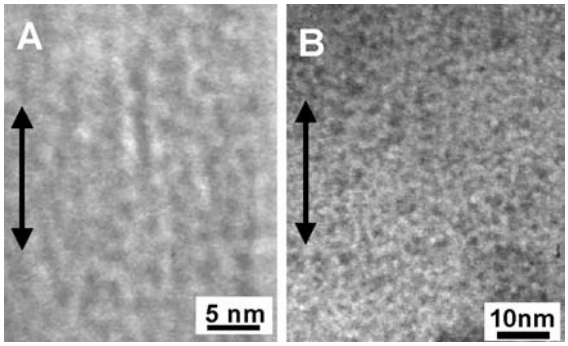

Figure 7. HRTEM images of single β-glucan chains in the ordered structure in the stretched water-swollen gel films at the drawing ratio of 2.0 of (A) α-chitin and (B) cellulose/α-chitin (25/75) blend. The double arrows indicate the stretching direction.

in comparison of NOC data. The crystal lattice parameters for native crystalline α-chitin were reported as $a = 0.474$ nm, $b = 1.886$ nm, $c = 1.032$ nm, and $\alpha = \beta = \gamma = 90^\circ$ (Minke and Blackwell 1978). Since the average distance between any two lines in well-ordered states in Figure 7A was 1.88 ± 0.27 nm, this value coincides with the lattice dimension of the b axis. Therefore, considering that the stretching direction corresponds to the molecular chain axis (c-axis), the top view of the TEM image of Figure 7A indicates that the b–c plane of α-chitin microfibril may be aligned parallel as white lines with a distance of 1.62 ± 0.21 nm on the surface. In other words, by the same preparation method for NOC, α-chitin molecules may be self-assembled to form a microfibril, and further the individual microfibrils tend to be parallel with a distance of 1.62 ± 0.21 nm.

NOC/α-chitin blends

Figure 7B and the corresponding data in Table 2 exhibit a case of the stretched film of the cellulose/α-chitin blend with a composition of 75/25 (w/w) in the same manner as for NOC. The white dots or lines in Figure 7B indicate molecular chains or molecular aggregates, since the sample was negatively stained with uranium acetate for high-resolution TEM observation. Some parts are well oriented parallel to the stretching direction, and the molecular aggregates are entirely ordered along the stretching axis. The average line width as shown in Table 2 was narrower than that for nematic ordered pure α-chitin, indicating that the intermolecular interaction between cellulose and α-chitin may be engaged. Possibly each molecular chain is facing with each other against the surface by a hydrophobic interaction such as a van der Waals force. On the other hand, the average distance between two parallel lines was not significantly different between the two stretched films from α-chitin and the cellulose/α-chitin blend. Therefore, it is considered that the cellulose/α-chitin molecular aggregates in the stretched film are aligned similarly to nematic ordered α-chitin.

To deal with the above case in comparison of the NOC, we employed WAXD measurements in order to understand the molecular ordering occurring during stretching of the blended films of the water-swollen cellulose/α-chitin (50/50) gel. Figure 8 shows WAXD photographs for the stretched cellulose/α-chitin (50/50) films at the desired drawn ratio. When compared with that for cellulose shown in Figure 1, clearer Debye rings appeared even in undrawn films after being dried. Like the cellulose case, with increasing drawing ratio of the samples, the rings were becoming arcs in the equatorial direction. Similarly, such arcs appeared also at the meridional direction. WAXD intensity curves in both directions of Figure 9 indicate more clearly that some ordered crystallites, to some extent, were formed prior to stretching. Through the stretching, the two peaks at $2\theta = 9.3$ and 19.5 in the equatorial direction were becoming narrower and sharper, while the meridional reflections were not significantly changed after the stretching. These results indicate that the intermolecular interaction between cellulose and α-chitin may cause molecular aggregations leading to some crystallization, and as a result, crystallites with a certain size were formed. Then, by stretching, the crystallites tend to be ordered parallel to the drawing axis.

Table 2. The average width and distance between two parallel lines analyzed by TEM images.

	Cellulose*	α-Chitin	Cellulose/α-Chitin 75/25
Line width	0.46 ± 0.05 (chain width)	1.88 ± 0.27	1.38 ± 0.18
Distance between two lines	0.66 ± 0.07	1.62 ± 0.21	1.65 ± 0.27

*From reference Kondo et al. (2001).

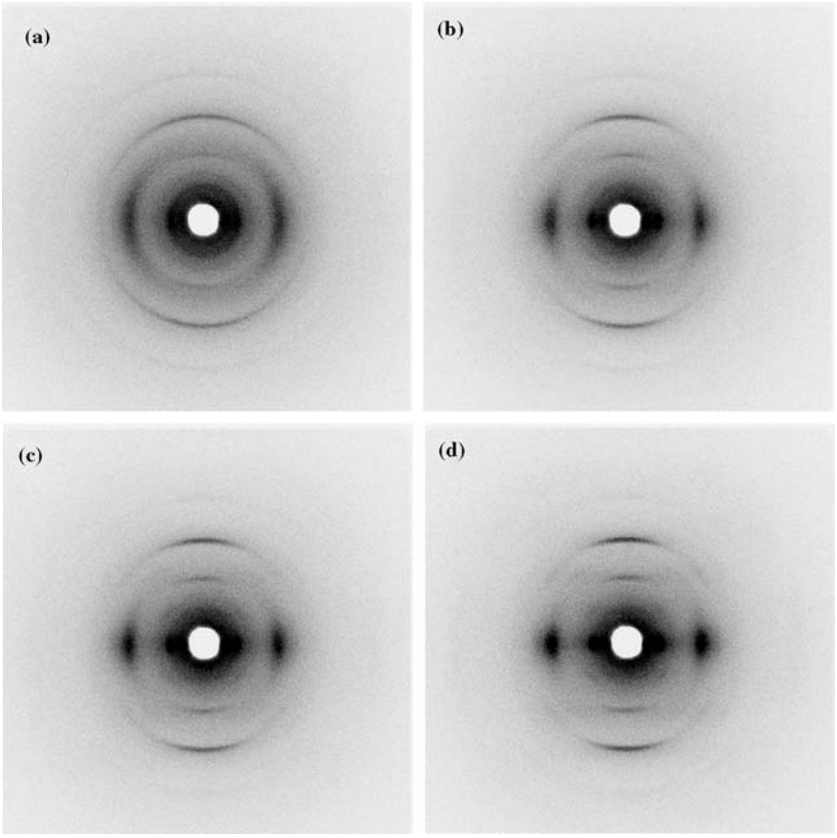

Figure 8. WAXD photographs for stretched cellulose/α-chitin (50/50) blended films at the desired drawn ratio: (a) undrawn water-swollen film after being dried at a fixed state; (b) drawn ratio 1.5; (c) drawn ratio 1.7; and (d) drawn ratio 2.0.

However, the stretching effect in ordering of the cellulose and α-chitin blends was slight when compared with nematic ordered pure cellulose or pure α-chitin. In particular, changes in the surface morphology of the blended samples evidently proved to be slight, as shown in AFM images of Figure 10. The corresponding data in Table 1 support that the change was not quantitatively large. This phenomenon may be attributed to the miscibility of the blend components, say polymer–polymer interaction.

The series of α-chitin used as a component for preparation of nematic ordered states have indicated that unlike NOC, at first the molecules tend

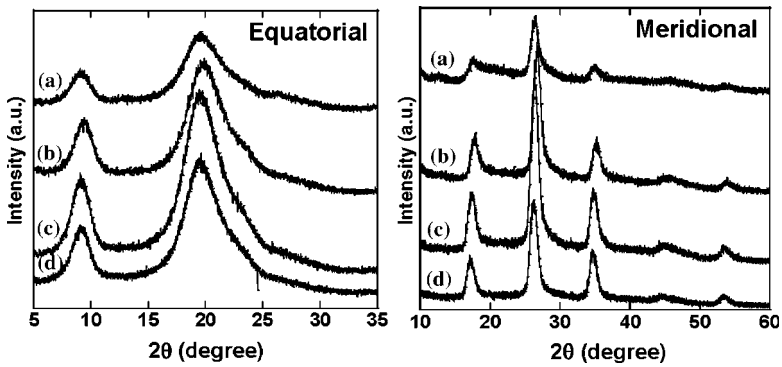

Figure 9. Equatorial (left) and meridional (right) intensity curves of the WAXD for cellulose/α-chitin (50/50) blended films stretched at the desired drawn ratio corresponding to (a)–(d) in Figure 8. The term 'a.u.' indicates arbitrary unit.

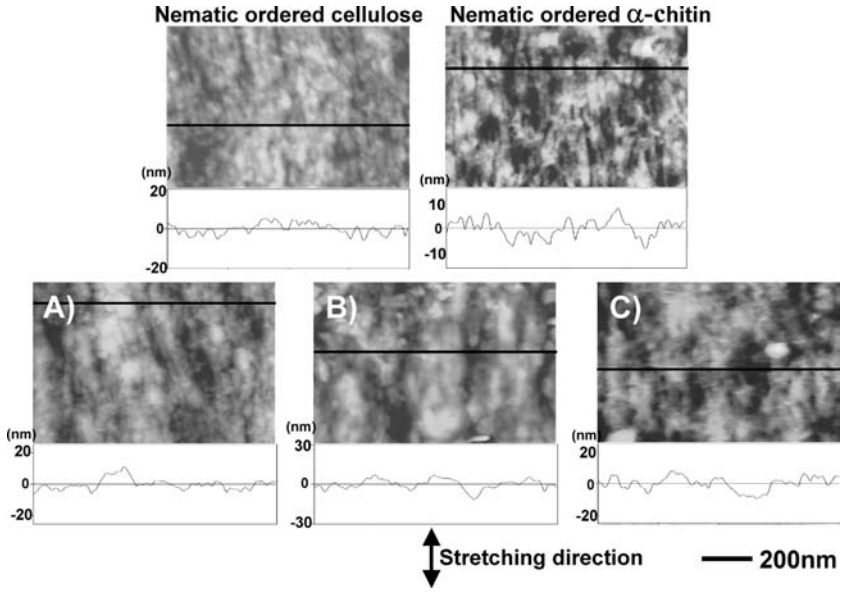

Figure 10. AFM images of height mode with the cross-section for cellulose/α-chitin (50/50) blended films stretched at the desired drawn ratio corresponding to (b)–(d) in Figure 8. The scale bar indicates 200 nm.

to be aggregated prior to stretching, and then by the stretching the nematic ordered states of the aggregates were formed.

Conclusions

In a previous paper, we emphasized that in categorizing the states of cellulose molecular association, it may be advantageous to first prioritize whether or not the cellulose is in the ordered or non-ordered domain, rather than determine if it is crystalline or non-crystalline. Then a unique form of cellulose, NOC, which was molecularly ordered, yet non-crystalline was proposed. Therefore, in this article, we attempted to clarify how β-glucan chains are assembled to form NOC during the stretching process. High-resolution TEM images proved that the molecular chains tend to be oriented along the stretching axis by uniaxial drawing. In addition, to transfer the physical force to the molecules, the junction zones for the action may be required. The presence was proved by TEM images shown (in this paper) as well as FTIR measurements with deuteration of hydroxyl groups (Kondo et al. 2001). Now, if the number of zones can be artificially controlled, it would yield a variety of nematic ordered states that is ordered, yet non-crystalline.

We also wish to extend the concept of NOC to the nematic ordered states in other carbohydrate polymers. In this respect, α-chitin and cellulose/α-chitin blends were employed. Unlike the occurrence of molecular association for NOC, nematic ordered α-chitin and cellulose/α-chitin blends exhibited totally different features. Because of the strong association for α-chitin alone and between cellulose and α-chitin, molecular aggregations were formed prior to stretching. Thus, such an aggregation, instead of the individual molecular chains, led to nematic ordered states by uniaxial stretching of the precursor gel films. This result indicates that in the same manner as for NOC a variety of ordering at various scales is possibly formed, depending on the starting polymer materials.

Acknowledgements

We thank Mr Eiji Togawa at Forestry and Forest Products Research Institute (F.F.P.R.I.) for his technical assistance with X-ray measurements. We also thank Dr Yukie Saito at Graduate School of Agricultural and Life Sciences, The University of Tokyo for a valuable comment. This research was partly supported by a Grant-in-Aid for Scientific Research (No. 14360101), Japan Society for the

Promotion of Science (JSPS) and by the Welch Foundation (F-1217), and the Johnson & Johnson Centennial Chair Funds.

References

Harada H. and Côté W.A. Jr. 1985. In: Higuchi T. (ed.), Biosynthesis and Biodegradation of Wood Components. Academic Press, Orlando, Florida, p. 1.

Hishikawa Y., Togawa E., Kataoka Y. and Kondo T. 1999. Characterization of amorphous domains in cellulosic materials using a FTIR deuteration monitoring analysis. Polymer 40: 7117–7124.

Kageyama K., Tamazawa J. and Aida T. 1999. Extrusion of polymerization: catalyzed synthesis of crystalline linear polyethylene nanofibers within a mesoporous silica. Science 285: 2113–2115.

Kondo T. 1999. In: Argyropoulos D. (ed.), Advances in Lignocellulosics Characterization. Tappi Press, Atlanta, Georgia, p. 337, Chapter 14.

Kondo T., Nojiri M., Hishikawa Y., Togawa E., Romanovicz D. and Brown R.M. Jr. 2002. Biodirected epitaxial nanodeposition of polymers on oriented macromolecular templates. Proc. Natl. Acad. Sci. USA 99: 14008–14013.

Kondo T. and Sawatari C. 1996. A Fourier transform infra-red spectroscopic analysis of the character of hydrogen bonds in amorphous cellulose. Polymer 37: 393–399.

Kondo T., Togawa E. and Brown R.M. Jr. 2001. Nematic ordered cellulose: a concept of glucan chain association. Biomacromolecules 2: 1324–1330.

Matsuo M., Sawatari C., Iida M. and Yoneda M. 1985. Ultradrawing of high molecular weight polyethylene films produced by gelation/crystallization from solution: effect of the number of entanglements. Polym. J. 17: 1197–1208.

Minke R. and Blackwell J. 1978. The structure of α-chitin. J. Mol. Biol. 120: 167–181.

Saito Y., Okano T., Chanzy H. and Sugiyama J. 1995. Structural study of α-chitin from the grasping spines of the arrow worm (*Sagitta* spp.). J. Struct. Biol. 114: 218–228.

Togawa E. and Kondo T. 1999. Change of morphological properties in drawing water-swollen cellulose films prepared from organic solutions – a view of molecular orientation in the drawing process. J. Polym. Sci. B: Polym. Phys. 37: 451–459.

Wardrop A.B. 1964. In: Zimmermann M.H. (ed.), The Formation of Wood in Forest Trees. Academic Press, New York, p. 87.